Supporting Information

Colloidal $KLu_3F_{10}:Tb^{3+}$ persistent luminescence nanocrystals based flexible detector for 3D X-ray imaging

Fei Xie,[a] Dongxun Chen,[a] Yi Zhang,[a] Xulong Lv,[a] Xin Chen,*[b] Kangning Sun [a] and Yanjie Liang*[a]

[a]*Key Laboratory for Liquid-Solid Structure Evolution and Processing of Materials, Ministry of Education, Shandong University, Jinan 250061, China. E-mail: yanjie.liang@sdu.edu.cn.*

[b]*State Key Laboratory of Infrared Physics, Shanghai Institute of Technical Physics, Chinese Academy of Sciences, Shanghai 200083, China. E-mail: xinchen@mail.sitp.ac.cn.*

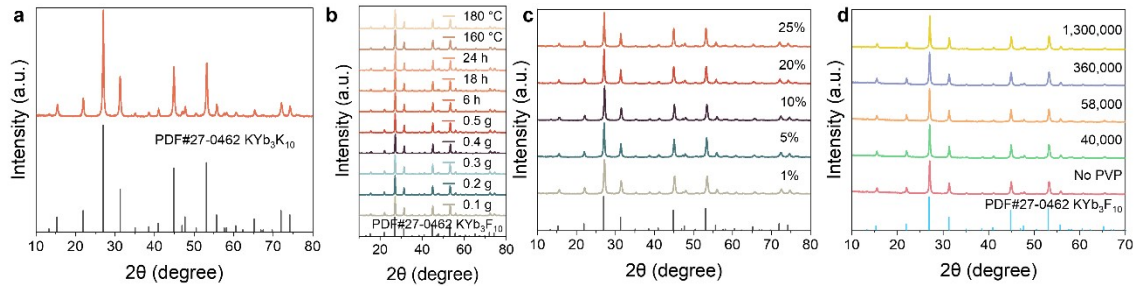

Fig. S1 XRD patterns of KLF:15%Tb a) doped with CA, b**)** doped with different contents of PVP surfactants, with different reaction temperatures and different reaction times, respectively, c**)** XRD patterns of KLF:x%Tb (x = 1, 5, 10, 20, 25), d) XRD pattern of KLF:15%Tb NCs mixed with PVP of different molecular weights.

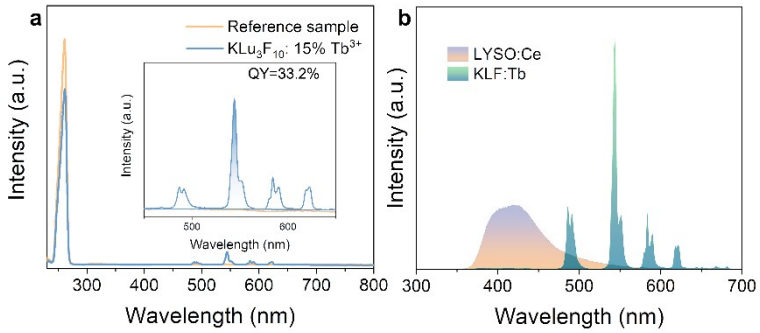

Fig. S2 (a) Excitation line of $BaSO_4$ and emission spectrum of KLu_3F_{10}: 15%Tb^{3+} sample. The inset shows the magnification of the emission spectrum. (b) Radioluminescence emission spectrum of LYSO:Ce and KLF:Tb under the same test detection.

The QE of the sample was calculated according to the following equation:

$$\eta_{QE} = \frac{\int L_S}{\int E_R - \int E_S}$$

Where η_{QE} represents the photoluminescence QE, L_S is the PL spectra of the sample, E_R and E_S are the photoluminescence excitation spectra of the excitation light with and without synthesized compound in the integrating sphere, respectively.

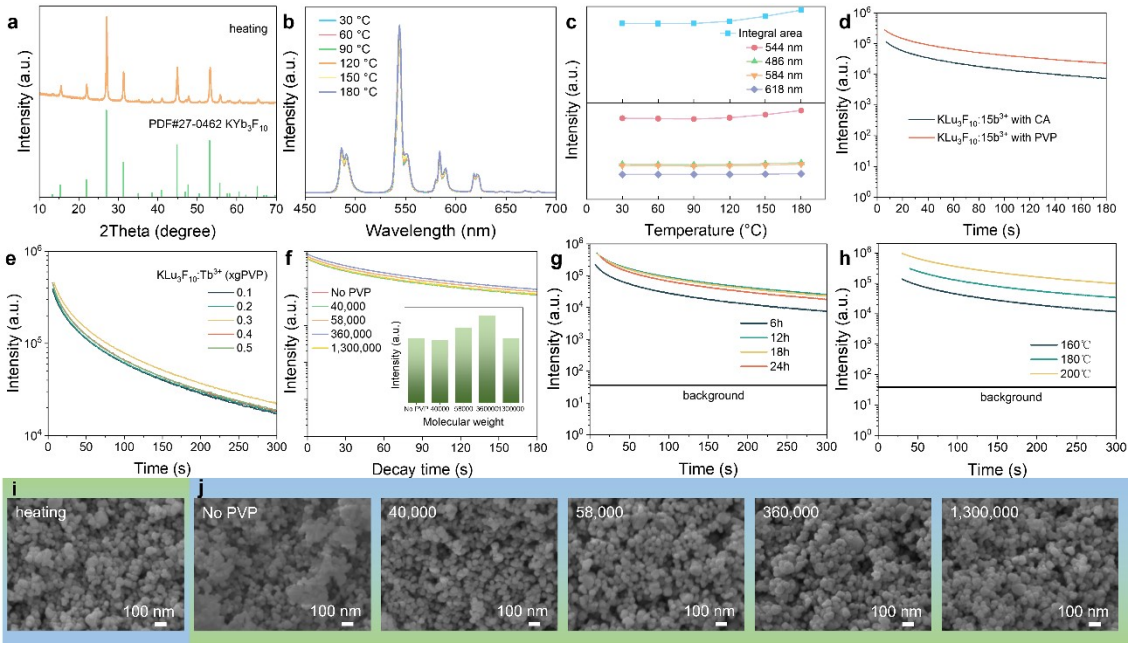

Fig. S3 (a) XRD patterns of the KLF:15%Tb NCs heated at 180 °C for three cycles. (b) Temperature-dependent emission spectra of the KLF:15%Tb NCs. (c) The luminescence intensity of KLF:15%Tb NCs monitored at 486 nm, 544 nm, 584 nm, and 618 nm, respectively, and the integral area of the whole emission spectrum. Afterglow curves of KLF:15%Tb d) doped with different surfactants, e) doped with different levels of PVP surfactants, f) mixed with PVP of different molecular weights and the inset shows the luminescence intensity monitored at 30 s, g) with different reaction times after 5 min of X-ray irradiation, and h) with different reaction temperatures. SEM images of the KLF:15%Tb NCs i) heated at 180 °C for three cycles, j) without and with PVP of different molecular weights.

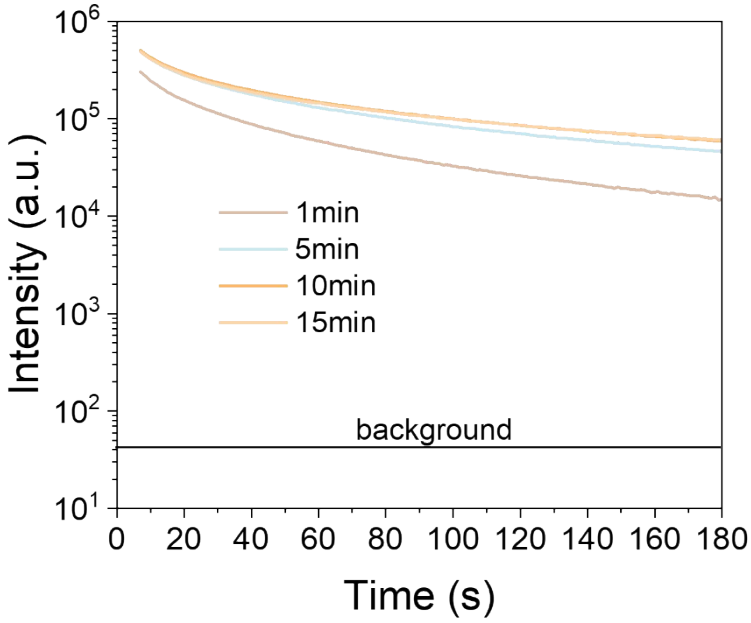

Fig. S4 Afterglow curves of the KLF:15%Tb at different X-ray irradiation times.

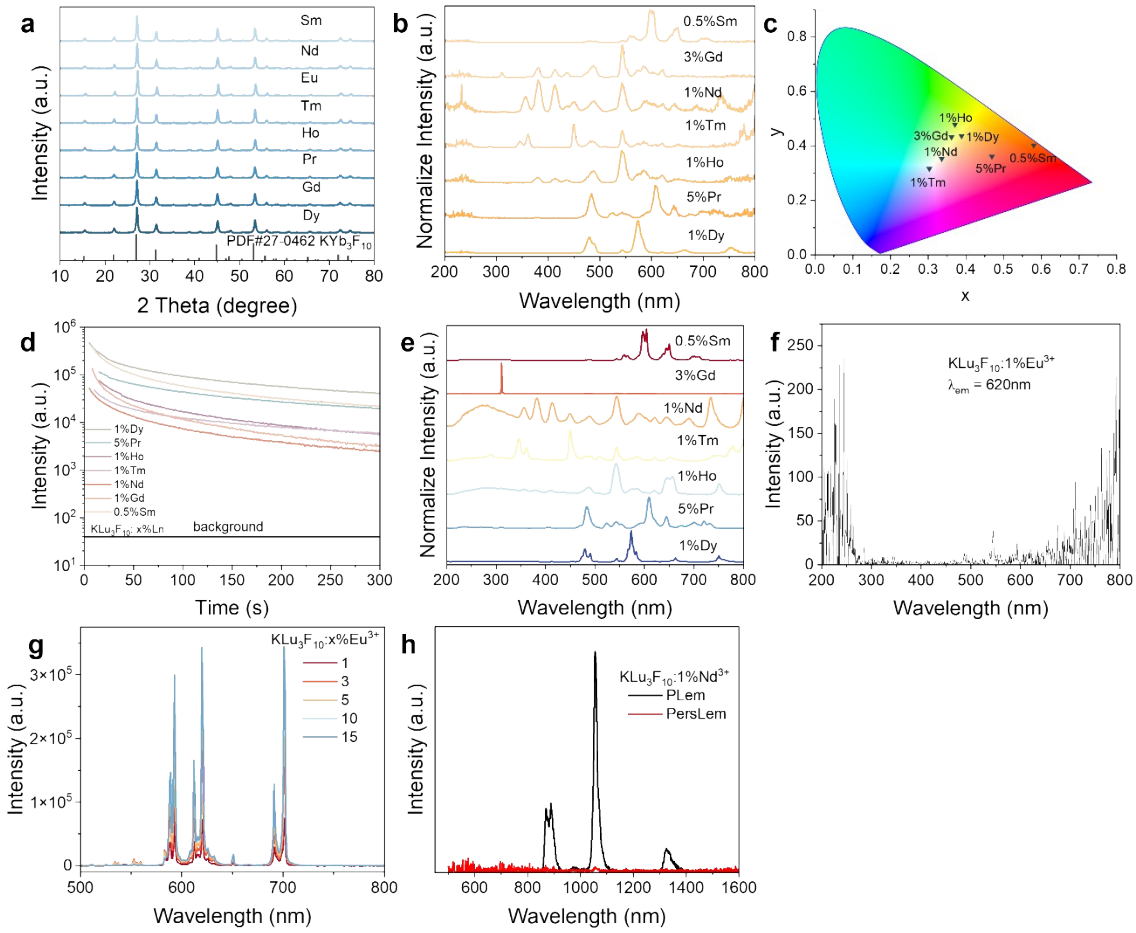

Fig. S5 XRD pattern (a), persistent luminescence spectra (b), cie chromaticity diagram (c), afterglow curve (d), radioluminescence spectra (e), of KLF:x%Ln (Sm, Gd, Nd, Tm, Ho, Pr, Dy). (f) persistent luminescence spectra of KLF:Eu^{3+}. (g) radioluminescence spectra of KLF:x%Eu^{3+} (x = 1, 3, 5, 10, 15). (h) radioluminescence and persistent luminescence spectra of KLF:Nd^{3+}.

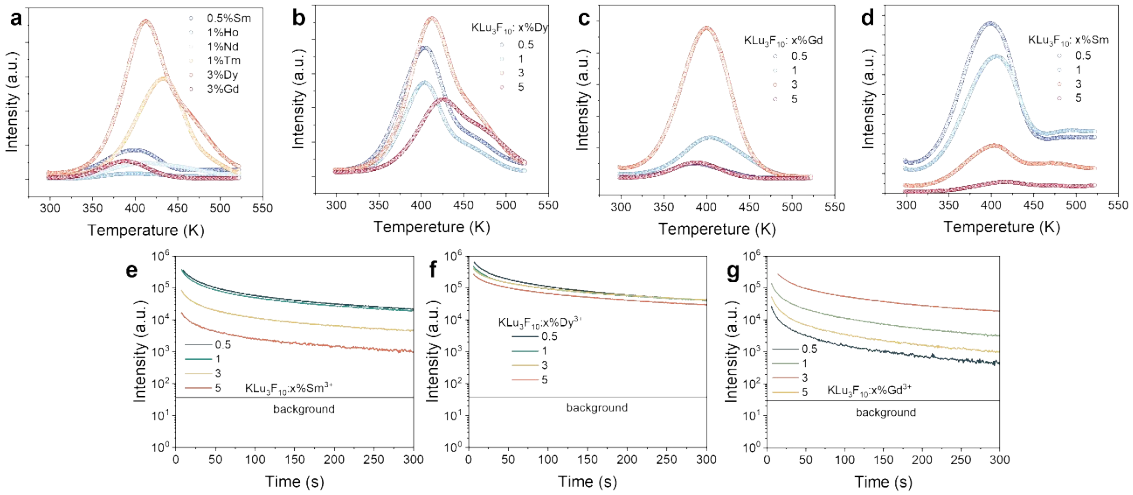

Fig. S6 TL curves of (a) KLF:Ln (Ln = Sm, Ho, Nd, Tm, Dy, Gd), (b) KLF:x%Dy (x = 0.5,1,3,5), (c) KLF:x%Gd (x = 0.5,1,3,5), (d) KLF:x%Sm (x = 0.5,1,3,5). e-g) Afterglow spectra of KLF:x%Sm/Dy/Gd (x = 0.5, 1, 3, 5).

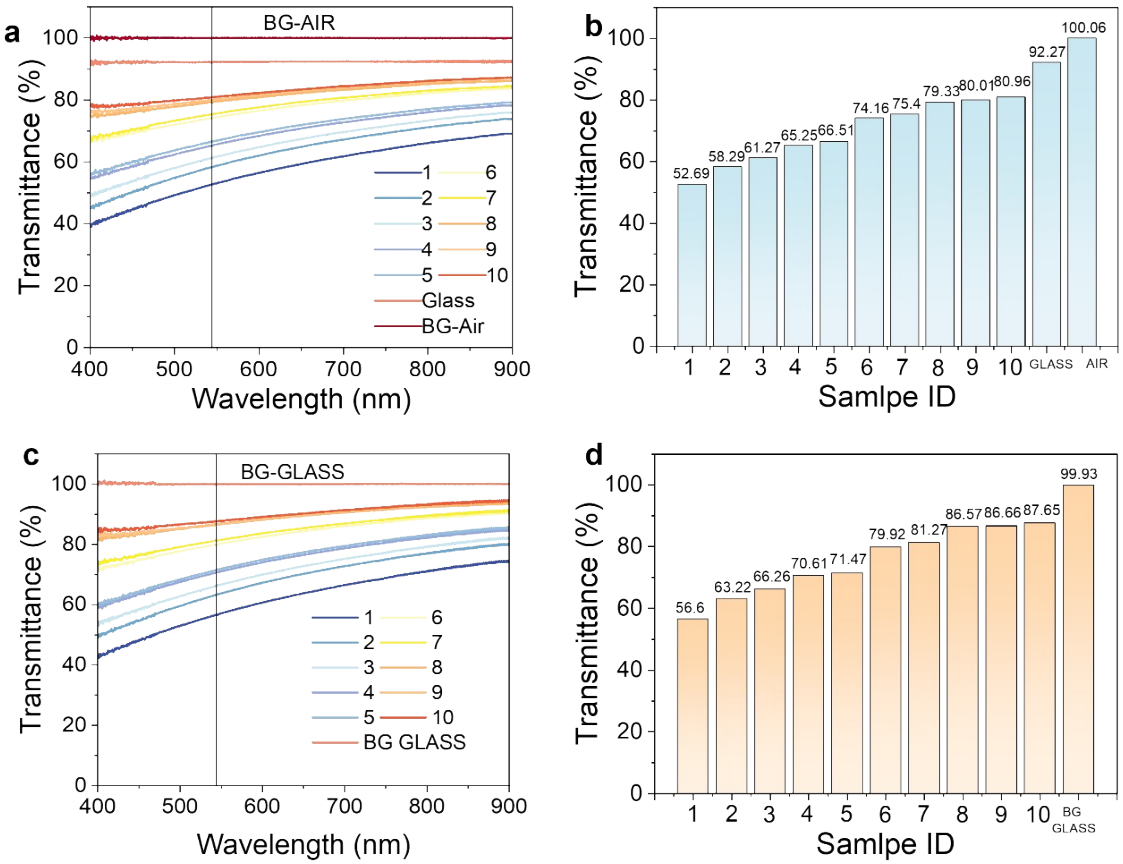

Fig. S7 (a) Transmittance curve of a samples film with glass as background. (b) Histogram of the transmittance of a sample film on a glass sheet at 544 nm.

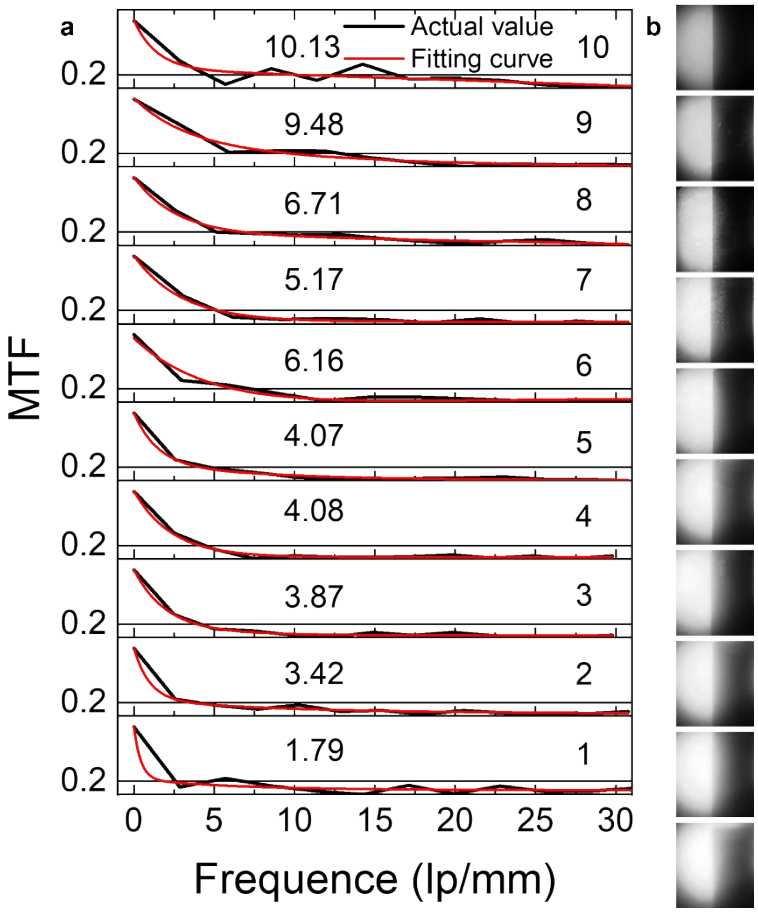

Fig. S8 (a) Fitting curves and actual value of MTF of films with different transmittance. (b) Photographs of the hypotenuse of films of different thicknesses.

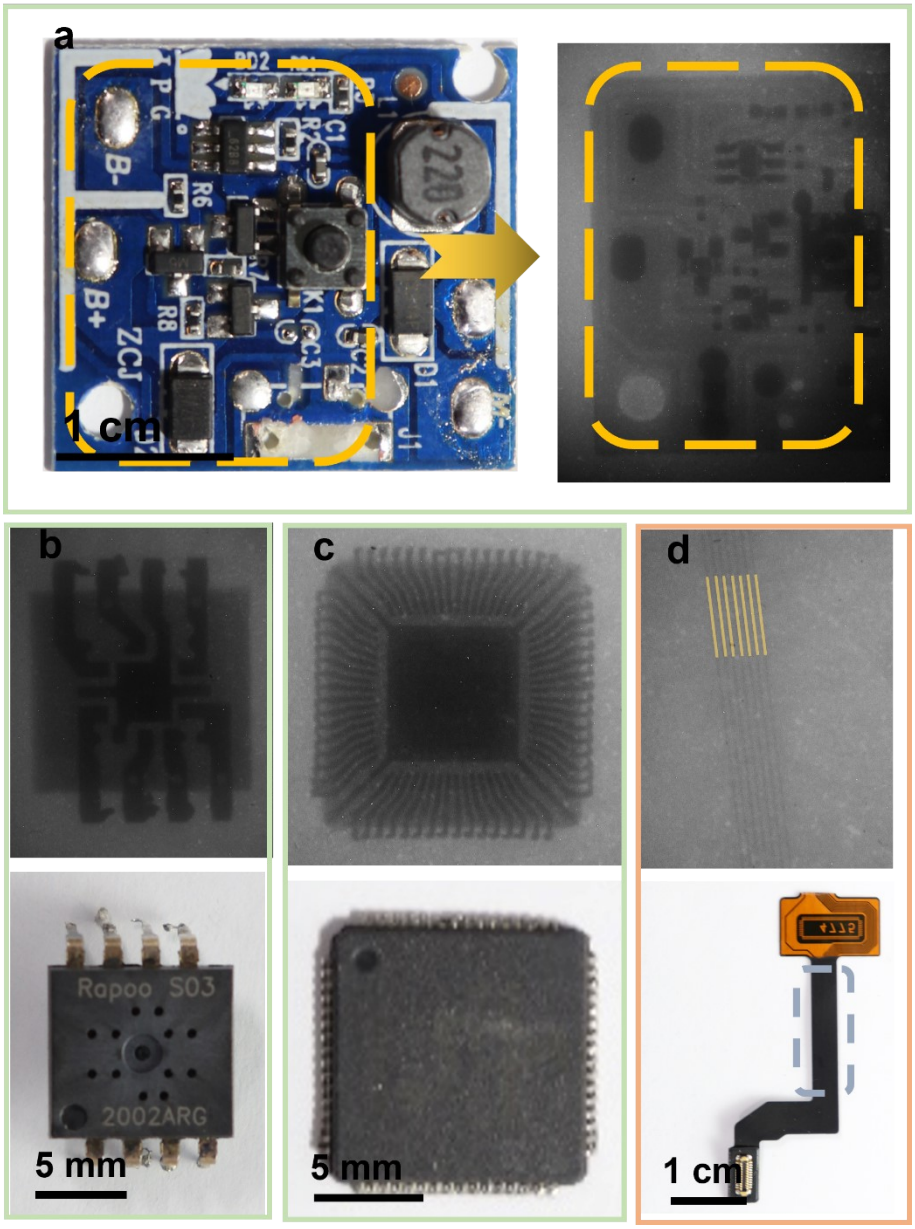

Fig. S9 (a) X-ray direct imaging of the circuit board. The yellow dotted box is selected as the imaging part. Photos of (b, c) electronic parts and components, and (d) flexible circuits recorded under room light and X-ray irradiation, respectively.